Eur. Phys. J. D **11**, 267–272 (2000)

THE EUROPEAN PHYSICAL JOURNAL D

EDP Sciences

Effects of quantum interference on the spontaneous emission in a coherently driven three-level atom

S. Yuan[a] and J.-Y. Gao

Department of physics, Jilin University, Changchun 130023, P.R. China

Received 8 September 1999 and Received in final form 13 January 2000

Abstract. A new scheme of the influence of quantum interference on the spontaneous emission in a coherently driven three-level medium is presented in this paper. The results are the same with that discussed by [S.-Y. Zhu, L.M. Narducci, M.O. Scully, Phys. Rev. A **52**, 4791 (1995)] under resonance conditions, but they are different when the driven field is detuned.

PACS. 42.50.Ct Quantum description of interaction of light and matter; related experiments – 42.50.Lc Quantum fluctuations, quantum noise, and quantum jumps

1 Introduction

Quantum interference in atomic systems in spontaneous emission can lead to many novel effects. Quenching of spontaneous emission [1–3] has been discussed for many years, where the coherence which is induced from spontaneous emission process is used for the preparation of the atom. Lately there are many related works in this field, including the modifications to spontaneous emission, resonance fluorescence, probe absorption spectra, and photon statistics [4–9], which are considered in V-type atoms [6–8], Λ-type atoms [9] and four-level atoms [5], respectively.

In this paper we investigate the effects of quantum interference on the spontaneous emission in a Σ-type atom – a model similar to reference [10], but with different coupling schemes. In reference [10], the spontaneous emission from the excited to the ground state when either of them is coupled to another excited state by a coherent field was discussed. In this paper, we study the spontaneous emission between two excited states when either of them is split into Autler-Townes doublets by the action of a coherent field. We find that the results are the same with that of reference [10] under resonance conditions, but they are different when the driven field is detuned.

2 Simplified models and spontaneous-emission spectra

The setting of interest is illustrated schematically in Figure 1. Because the calculation strategy is somewhat different in the two cases for reasons of convenience, we consider each separately and, for ease of nomenclature, we refer to the configuration of Figure 1a as the "upper level coupling" while we refer to that of Figure 1b as the "lower level coupling".

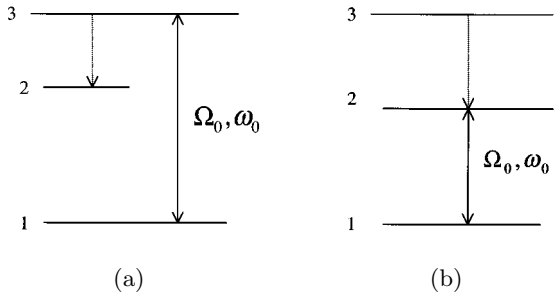

Fig. 1. Schematic representation of the atomic configurations discussed in this paper; (a) upper level coupling and (b) lower level coupling. In both cases Ω_0 denotes the Rabi frequency of the external driving field, and ω_0 its carrier frequency. The dotted line indicates the spontaneous decay process that generates the spectrum of interest.

In the setting of Figure 1a: the excited atomic state of interest, level 3, is coupled by a coherent field to another level of the atom, level 1 in this case, and it undergoes spontaneous emission to the level 2 as a result of the interaction of the atom with the vacuum. The second situation is illustrated schematically in Figure 1b: the atomic level 2 is coupled by the coherent field to the level 1, while level 3 decays to the level 2 by spontaneous emission. In the two simplified models we ignore both the mechanism by which the atom is placed in its initial excited state and the spontaneous relaxation of the atom from level 3 and level 2 to level 1.

[a] e-mail: qol@mail.jlu.edu.cn

2.1 Upper level coupling

With reference to Figure 1a, in the interaction picture the Schrödinger equation for the driven atom is

$$\frac{\mathrm{d}}{\mathrm{d}t}\left|\Psi(t)\right\rangle = -\frac{\mathrm{i}}{\hbar}H_I\left|\Psi(t)\right\rangle \tag{1}$$

where

$$H_I(t) = \mathrm{i}\hbar\sum_j g_j(\mathrm{e}^{-\mathrm{i}\delta_j t}b_j a_3^+ a_2 - \mathrm{e}^{\mathrm{i}\delta_j t}b_j^+ a_2^+ a_3) + \mathrm{i}\hbar(\Omega_0\mathrm{e}^{-\mathrm{i}\Delta_0 t}a_3^+ a_1 - \Omega_0^*\mathrm{e}^{\mathrm{i}\Delta_0 t}a_1^+ a_3) \tag{2}$$

and where the detuning parameters δ_j, Δ_0 are defined by

$$\delta_j = \omega_j - \omega_{32}, \quad \Delta_0 = \omega_0 - \omega_{31}. \tag{3}$$

We assume that the state vector of the system at time t have the form

$$\left|\Psi(t)\right\rangle = C_1(t)\left|0\right\rangle\left|1\right\rangle + C_3(t)\left|0\right\rangle\left|3\right\rangle + \sum_j C_{2j}(t)b_j^+\left|0\right\rangle\left|2\right\rangle \tag{4}$$

where $|0\rangle$ denotes the vacuum of the electromagnetic field, and the initial values of the expansion amplitudes are $C_{2j}(0) = 0$, and $C_1(0)$, $C_3(0)$ are arbitrary (apart, of course, for the normalization requirement).

Upon substituting equation (4) into equation (1) and after some simple steps, we arrive at the following first-order differential equations for the expansion amplitudes:

$$\dot{C}_{2j}\,(t) = -g_j\mathrm{e}^{\mathrm{i}\delta_j t}C_3(t) \tag{5a}$$

$$\dot{C}_3\,(t) = \Omega_0\mathrm{e}^{-\mathrm{i}\Delta_0 t}C_1(t) + \sum_{j=1}^{\infty} g_j\mathrm{e}^{-\mathrm{i}\delta_j t}C_{2j}(t) \tag{5b}$$

$$\dot{C}_1\,(t) = -\Omega_0^*\mathrm{e}^{\mathrm{i}\Delta_0 t}C_3(t) \tag{5c}$$

which we can solve along the lines of the traditional approach of Weisskopf and Wigner [11], as shown in some detail in Appendix. The initial conditions are

$$C_3(0) = 1, \quad C_1(0) = 0. \tag{6}$$

The required results are

$$C_1(t\to\infty) = 0 \tag{7a}$$

$$C_3(t\to\infty) = 0 \tag{7b}$$

$$C_{2j}(t\to\infty) = \frac{\mathrm{i}(\delta_j - \Delta_0)}{[|\Omega_0|^2 - \delta_j^2 + \Delta_0\delta_j - \mathrm{i}\gamma(\delta_j - \Delta_0)/2]} \tag{7c}$$

where $\gamma = 2\pi D(\omega_{32})g^2(\omega_{32})$, $D(\omega_{32})$ is the vacuum density of models calculated at the atomic transition frequency. In this calculation we have ignored the small vacuum-induced frequency shift at the transition frequency ω_{32}.

The spontaneous-emission spectrum, $S(\omega)$, is proportional to the Fourier transform of the field correlation function

$$\left\langle E^{(-)}(r,t+\tau)E^{(+)}(r,t)\right\rangle_{t\to\infty} = \left\langle\Psi(t)\mid E^{(-)}(r,t+\tau)E^{(+)}(r,t)\mid\Psi(t)\right\rangle_{t\to\infty} \tag{8}$$

where, in a finite quantization volume, the positive and negative frequency parts of the electric field operator are given, respectively, by

$$E^{(+)}(r,t) = \mathrm{i}\sum_{j=1}^{\infty}\left(\frac{\hbar\omega_j}{2\varepsilon_0 V}\right)^{1/2}\varepsilon_j b_j\exp[\mathrm{i}(K_j r - \omega_j t)] \tag{9a}$$

$$E^{(-)}(r,t) = \left[E^{(+)}(r,t)\right]^+ \tag{9b}$$

and where the asymptotic form of the state vector is

$$\left|\Psi(t\to\infty)\right\rangle = \sum_{j=1}^{\infty}C_{2j}(\infty)b_j^+\left|0\right\rangle\left|2\right\rangle \tag{10}$$

with

$$\sum_j |C_{2j}(\infty)|^2 = 1. \tag{11}$$

After substituting equations (9a, 9b, 7c) into equation (8), and after carrying out the infinite volume limit, we arrive at the required result

$$S(\omega) \propto |C_{2,\omega}|^2 = g^2\frac{(\delta - \Delta_0)^2}{(\delta^2 - \delta\Delta_0 - |\Omega_0|^2)^2 + (\gamma/2)^2(\delta - \Delta_0)^2} \tag{12}$$

with δ_j replaced by $\delta = \omega - \omega_{32}$ in equation (7c).

2.2 Lower level coupling

For the setting illustrated in Figure 1b, we introduce the dressed atomic eigenstates $|\alpha\rangle$ and $|\beta\rangle$ in the interaction picture, defined by

$$\left|\alpha\right\rangle = \mathrm{i}\mathrm{e}^{\mathrm{i}\Phi}\sin\theta\left|1\right\rangle + \cos\theta\left|2\right\rangle,$$
$$\left|\beta\right\rangle = -\mathrm{i}\mathrm{e}^{-\mathrm{i}\Phi}\cos\theta\left|1\right\rangle + \sin\theta\left|2\right\rangle \tag{13}$$

where

$$\Omega_0 = |\Omega_0|\,\mathrm{e}^{\mathrm{i}\Phi} \tag{14a}$$

$$\sin\theta = \frac{|\Omega_0|}{\sqrt{\lambda_\alpha^2 + |\Omega_0|^2}} \tag{14b}$$

$$\cos\theta = \frac{|\Omega_0|}{\sqrt{\lambda_\beta^2 + |\Omega_0|^2}} \tag{14c}$$

and the corresponding eigenvalues λ_α and λ_β are given by

$$\lambda_\alpha = -\frac{\Delta_0}{2} + (\frac{\Delta_0^2}{4} + |\Omega_0|^2)^{\frac{1}{2}}, \tag{15a}$$

$$\lambda_\beta = -\frac{\Delta_0}{2} - (\frac{\Delta_0^2}{4} + |\Omega_0|^2)^{\frac{1}{2}}. \tag{15b}$$

The initial conditions $C_3(0) = 1$, $\alpha_j(0) = \beta_j(0) = 0$, for all values of j. After simple calculation as done in Section 2.1, the asymptotic form of the state vector can be expressed as

$$|\Psi(t \to \infty)\rangle = \sum_j \alpha_j(t) b_j^+ |0\rangle |\alpha\rangle + \sum_j \beta_j(t) b_j^+ |0\rangle |\beta\rangle \tag{16}$$

where

$$\alpha_j(t \to \infty) = g \cos\theta \frac{\mathrm{e}^{-\mathrm{i}\lambda_\alpha t}}{\gamma/2 - \mathrm{i}(\lambda_\alpha + \delta_j + \Delta_0)} \tag{17a}$$

$$\beta_j(t \to \infty) = g \sin\theta \frac{\mathrm{e}^{-\mathrm{i}\lambda_\beta t}}{\gamma/2 - \mathrm{i}(\lambda_\beta + \delta_j + \Delta_0)} \tag{17b}$$

with

$$\gamma = 2\pi[\cos^2\theta D(\omega_{32} - \lambda_\alpha) g^2(\omega_{32} - \lambda_\alpha) + \sin^2\theta D(\omega_{32} - \lambda_\beta) g^2(\omega_{32} - \lambda_\beta)]. \tag{18}$$

The spectrum of the spontaneously emitted light is

$$S(\omega) \propto \left(|\alpha_\omega(\infty)|^2 + |\beta_\omega(\infty)|^2\right) = \frac{\cos^2\theta}{(\gamma/2)^2 + (\delta + \Delta_0 + \lambda_\alpha)^2} + \frac{\sin^2\theta}{(\gamma/2)^2 + (\delta + \Delta_0 + \lambda_\beta)^2} \tag{19}$$

with δ_j replaced by $\delta = \omega - \omega_{32}$.

3 Discussion of the analytic results

While greatly simplified in nature, the models discussed in the preceding section contain the essential physical features that we wish to emphasize in this paper.

In the case of upper level coupling when the driving field is at the resonance with the 3–1 transition, the equation (12) shows that the emission line is split symmetrically around $\delta = 0$; the two side lobes have equal heights and the maxims are located at $\delta = \pm|\Omega_0|$. Furthermore, the full width at half maximum of each of the side lobes is given approximately by

$$\Delta\omega = \frac{1}{2}\gamma(1 + \frac{|\Omega_0|^2}{(\gamma/2)^2}) + 0(|\Omega_0|^4) \tag{20}$$

in the limit in which $|\Omega_0| \ll \gamma/2$. Hence, it follows that in the presence of a coherent driving field, even with an arbitrarily small amplitude and detuning, the emission spectrum is split into two parts. Two examples are shown in Figure 2 under resonance conditions for two different values of the driving field strength (note that in all the spectral displays, for simplicity, we have set the coupling constant g equal to unity).

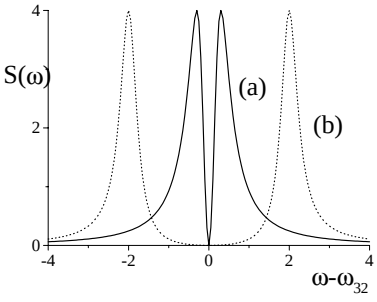

Fig. 2. Spontaneous emission spectrum $S(\omega)$ for the upper level coupling case with $\Delta_0 = 0$, $\gamma = 1.0$ and (a) $\Omega_0 = 0.3$, (b) $\Omega_0 = 3.0$.

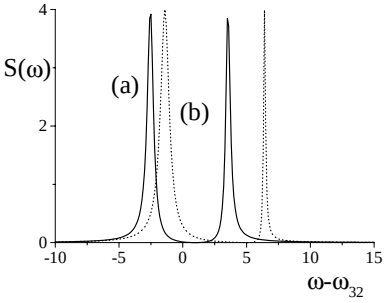

Fig. 3. Spontaneous emission spectrum $S(\omega)$ for the upper level coupling case with $\Omega_0 = 3$, $\gamma = 1.0$ and (a) $\Delta_0 = 1.0$, (b) $\Delta_0 = 5.0$.

When the driving field is detuned away from the ω_{31} transition frequency, the effect is illustrated in Figure 3 for a fixed value of the driving field Rabi frequency and two different positive values of the detuning parameter Δ_0. This figure shows that while the peak heights of the two spectral components remain the same, an increase of $\Delta_0 > 0$ broadens the width of the left half of the spectrum and narrows the width of the spectral component on the right one. The situation is reversed, relative to the origin of the frequency axis, if the detuning parameter is negative. In the limit in which $|\Delta_0| \gg |\Omega_0|$, the full widths at half maximum of the right and left peaks in Figure 3 are given approximately by

$$\Delta\omega_{\mathrm{R}} \approx \frac{1}{2}\gamma\frac{|\Omega_0|^2}{\Delta_0^2}, \quad \Delta\omega_{\mathrm{L}} \approx \frac{1}{2}\gamma\left(1 - \frac{|\Omega_0|^2}{\Delta_0^2}\right) \tag{21}$$

(the subscripts R and L in Eq. (8) denote right and left, respectively).

In the case of the lower level coupling (Fig. 1b), the fluorescence spectrum is the incoherent sum of two Lorentzian lines, see equation (19), each component has a full width at half maximum, γ. On resonance, the two lines have the same heights, as illustrated in Figure 4, while out of resonance one of the lines becomes more intense relative to the other (see Fig. 5).

Under resonance conditions, when the strength of the driving field decreases and eventually approaches zero, the frequency spacing between the dressed doublets vanishes for both cases. It is clear that, eventually, the spectra in both the upper and lower coupling schemes will have to approach the usual Lorentzian distribution function. This is true, indeed, but their approach to the Lorentzian shape is very different. In the case illustrated in Figure 1a the

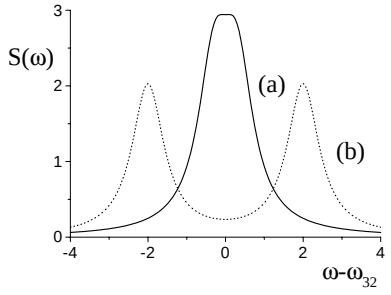

Fig. 4. Spontaneous emission spectrum $S(\omega)$ for the lower level coupling case with $\Delta_0 = 0$, $\gamma = 1.0$ and (a) $\Omega_0 = 0.3$, (b) $\Omega_0 = 2.0$.

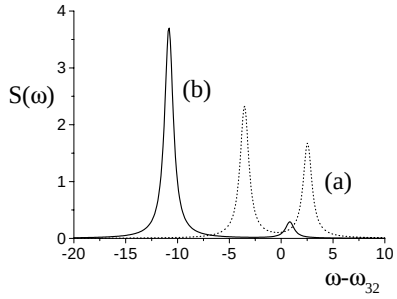

Fig. 5. Spontaneous emission spectrum $S(\omega)$ for the lower level coupling case with $\Omega_0 = 3$, $\gamma = 1.0$ and (a) $\Delta_0 = 1.0$, (b) $\Delta_0 = 10$.

spectrum is always split into two side lobes with a dark in the middle, which disappears only in the absence of the coherent driving field, as shown by curve (a) in Figure 2. In the case of the lower level coupling, as the Rabi frequency of the driving field decrease, the dip that separates the two side lobes becomes smaller until, eventually, it disappears when $|\Omega_0|$ becomes of the order of a few tenths of γ for $\Delta_0 = 0$ (see curve (a) of Fig. 4).

When the magnitude of the detuning parameter Δ_0 increases, the spontaneous-emission spectra are again to approach a Lorentzian shape, as the effect of the driving field becomes less and less pronounced. This continues to be true in both cases, but the approach to the Lorentzian emission line is again very different for the two models. This is apparent from the results shown in Figures 3 and 5.

We must stress that these results apply, strictly speaking, only to the idealized models analyzed in Section 2, where we have ignored the effects of the pumping mechanisms which are needed to prepare the atoms in their initial state, and the possible influence of additional competing decays. These effects will be described in more detail in the following section.

4 A more realistic model

It is surely not too realistic to expect that the atom can be placed in its initial excited state just at it enters the interaction region. What can be accomplished more easily in a practical setting is to let the interaction of the atoms with the driving fields begin at some arbitrary time, for example when an atom from an atomic beam enters the region occupied by the driving fields, and then to monitor the fluorescence spectrum under steady-state conditions, as done typically in resonance fluorescence studies.

For this purpose we consider an extension of the models illustrated in Figures 1a and 1b, which includes a second coherent driving field, Ω_1, at or near resonance with the 2–3 transition and also an incoherent pump mechanism characterized by a pump rate W_{23}. The reason for these modifications is to monitor explicitly the effect of the pumping process on the pure interference effect. Furthermore, we also include the remaining spontaneous decay processes at the rates W_{ij}, where i is the starting and j is the terminal level of the decay. The coherent driving field, which is already part of the simplified models, continues to be applied to the same pair of level and to be denoted by the Rabi frequency Ω_0.

It is no longer practically feasible to handle the extended models by the Weisskopf-Wigner method (state vector method). It is much easier, instead, to describe the atomic evolution by the standard master equation approach and to derive expressions for the spontaneous emission spectra with the help of the regression theorem [12]. The drawback of the increased generality of the models is that it is no longer possible to identify by inspection the terms responsible for quantum interference, although their presence is obvious from the final numerical results.

We begin with the upper level coupling case. In the presence of a second coherent driving field connecting levels 2 and 3 of Figure 1a the interaction Hamiltonian in the interaction representation takes the form

$$H_I(t) = -\hbar\Delta_0 |3\rangle\langle 3| - \hbar(\Delta_0 - \Delta_1)|2\rangle\langle 2| + \mathrm{i}\hbar(\Omega_0 |3\rangle\langle 1| - \Omega_0^* |1\rangle\langle 3|) + \mathrm{i}\hbar(\Omega_1 |3\rangle\langle 2| - \Omega_1^* |2\rangle\langle 3|) \tag{22}$$

where Δ_0 is defined as in equation (3), and

$$\Delta_1 = \omega_1 - \omega_{32}. \tag{23}$$

The calculation is based on the master equation and the regression theorem along the lines of reference [13]. The relevant equations of motion for the matrix elements of the density operator (in the interaction representation) can be written in the form

$$\frac{\mathrm{d}}{\mathrm{d}t}\Psi = L\Psi + I \tag{24}$$

where

$$\Psi_1 = \rho_{12}, \quad \Psi_2 = \rho_{13}, \quad \Psi_3 = \rho_{21}, \quad \Psi_4 = \rho_{22}, \quad \Psi_5 = \rho_{23}, \quad \Psi_6 = \rho_{31}, \quad \Psi_7 = \rho_{32}, \quad \Psi_8 = \rho_{33}. \tag{25}$$

The matrix L has the explicit form

$$L = \begin{pmatrix} -\Gamma_{12} & -\Omega_1 & 0 & 0 & 0 & 0 & -\Omega_0^* & 0 \\ \Omega_1^* & -\Gamma_{13} & 0 & -\Omega_0^* & 0 & 0 & 0 & -2\Omega_0^* \\ 0 & 0 & -\Gamma_{21} & 0 & -\Omega_0 & -\Omega_1^* & 0 & 0 \\ 0 & 0 & 0 & -W_{21} - W_{23} & -\Omega_1 & 0 & -\Omega_1^* & 0 \\ 0 & 0 & \Omega_0^* & \Omega_1^* & -\Gamma_{23} & 0 & 0 & -\Omega_1^* \\ 0 & 0 & \Omega_1 & -\Omega_0 & 0 & -\Gamma_{31} & 0 & -2\Omega_1 \\ \Omega_0 & 0 & 0 & \Omega_1 & 0 & 0 & -\Gamma_{32} & -\Omega_1 \\ 0 & \Omega_0 & 0 & W_{23} & \Omega_1 & \Omega_0^* & \Omega_1^* & -W_{32} - W_{31} \end{pmatrix} \tag{26}$$

where

$$\begin{aligned}
&\Gamma_{12} = \gamma_{12} + \mathrm{i}(\Delta_0 - \Delta_1), \quad \Gamma_{13} = \gamma_{13} + \mathrm{i}\Delta_0,\\
&\Gamma_{21} = \gamma_{21} - \mathrm{i}(\Delta_0 - \Delta_1), \quad \Gamma_{23} = \gamma_{23} + \mathrm{i}\Delta_0,\\
&\Gamma_{31} = \gamma_{31} - \mathrm{i}\Delta_0, \qquad\qquad \Gamma_{32} = \gamma_{32} - \mathrm{i}\Delta_0, \qquad (27)
\end{aligned}$$

$$\gamma_{ij} = \frac{1}{2}\sum_{k=1}^{3}(W_{ik} + W_{jk}) \qquad (28)$$

the inhomogeneous vector I has nonzero components

$$I_2 = \Omega_0^*, \quad I_6 = \Omega_0. \qquad (29)$$

The required spectrum is proportional to the Fourier transform of the two-time correlation function

$$\Gamma^{(1)}(t_1, t_0) = \left\langle P^{(-)}(t_1)P^{(+)}(t_0)\right\rangle \qquad (30)$$

where $P^{(+)} = \mu_{23}b_2^+ b_3, P^{(-)} = \left[P^{(+)}\right]^+$

Equation (24) must be calculated in steady state, *i.e.* under the double limit

$$t_0, \quad t_1 \to \infty, \quad t_1 - t_0 = \tau > 0 \qquad (31)$$

where τ is arbitrary. Following the same procedure as described in reference [13] leads to the result

$$\begin{aligned}
\Gamma^{(1)}(\tau) = \mu_{23}^2\Big[&\left(\mathrm{e}^{L\tau}\right)_{53}\Psi_6(\infty) + \left(\mathrm{e}^{L\tau}\right)_{54}\Psi_7(\infty)\\
&+ \left(\mathrm{e}^{L\tau}\right)_{55}\Psi_8(\infty) + \int_0^\tau \mathrm{d}\tau' \sum_{j=1}^{8}(\mathrm{e}^{L(\tau-\tau')})_{5j}I_j\Psi_7(\infty)\Big]
\end{aligned} \qquad (32)$$

where

$$\Psi_i(\infty) = -\sum_{j=1}^{8}(L^{-1})_{ij}I_j \qquad (33)$$

denotes the ith stationary matrix element of the density operator, according to the notations introduced in equation (25).

After elimination of the coherent part, the spectrum of the radiated fluorescence is given by

$$S(\omega) = \mathrm{Re}\,\overset{\wedge}{\Gamma}{}^{(1)}_{\mathrm{incoh}}(z)\mid_{z=\mathrm{i}\omega} \qquad (34)$$

where $\overset{\wedge}{\Gamma}{}^{(1)}_{\mathrm{incoh}}(z)$, the so-called incoherent part of the Laplace transform of $\Gamma^{(1)}(z)$, has the explicit form

$$\begin{aligned}
\overset{\wedge}{\Gamma}{}^{(1)}_{\mathrm{incoh}}(z) = &M_{53}(z)\Psi_6(\infty) + M_{54}(z)\Psi_7(\infty)\\
&+ M_{55}(z)\Psi_8(\infty) + \sum_{j=1}^{8}N_{5j}(z)I_j\Psi_7(\infty)
\end{aligned} \qquad (35)$$

and where

$$M_{ij}(z) = \left[(z-L)^{-1}\right]_{ij}, N_{ij}(z) = \left[L^{-1}(z-L)^{-1}\right]_{ij}. \qquad (36)$$

For the case of the lower level coupling the interaction Hamiltonian is given by

$$\begin{aligned}
H_I(t) = &-\hbar(\Delta_1 + \Delta_0)\left|3\right\rangle\left\langle 3\right| - \hbar\Delta_0\left|2\right\rangle\left\langle 2\right| + \mathrm{i}\hbar(\Omega_0\left|2\right\rangle\left\langle 1\right|\\
&- \Omega_0^*\left|1\right\rangle\left\langle 2\right|) + \mathrm{i}\hbar(\Omega_1\left|3\right\rangle\left\langle 2\right| - \Omega_1^*\left|2\right\rangle\left\langle 3\right|).
\end{aligned} \qquad (37)$$

With the same assignment of the components of the vector Ψ as given by equation (25), the new matrix L takes the form

$$L = \begin{pmatrix}
-\Gamma_{12} & -\Omega_1 & 0 & -\Omega_0^* & 0 & 0 & 0 & -\Omega_0^*\\
\Omega_1^* & -\Gamma_{13} & 0 & 0 & -\Omega_0 & 0 & 0 & 0\\
0 & 0 & -\Gamma_{21} & -2\Omega_0 & 0 & -\Omega_1 & 0 & -\Omega_1\\
\Omega_0 & 0 & -\Omega_0^* & -W_{21} - W_{23} & -\Omega_1 & 0 & -\Omega_1 & 0\\
0 & \Omega_0 & 0 & \Omega_1^* & -\Gamma_{23} & 0 & 0 & -\Omega_1^*\\
0 & 0 & \Omega_1 & 0 & 0 & -\Gamma_{31} & -\Omega_0 & 0\\
0 & 0 & 0 & \Omega_1 & 0 & \Omega_0^* & -\Gamma_{32} & -\Omega_1\\
0 & 0 & 0 & W_{23} & \Omega_1 & 0 & \Omega_1^* & -W_{32} - W_{31}
\end{pmatrix} \qquad (38)$$

where

$$\begin{aligned}
&\Gamma_{12} = \gamma_{12} + \mathrm{i}\Delta_0, \Gamma_{13} = \gamma_{13} + \mathrm{i}(\Delta_0 + \Delta_1), \Gamma_{21} = \gamma_{21} - \mathrm{i}\Delta_0,\\
&\Gamma_{23} = \gamma_{23} - \mathrm{i}\Delta_1, \Gamma_{31} = \gamma_{31} - \mathrm{i}(\Delta_0 + \Delta_1), \Gamma_{32} = \gamma_{32} - \mathrm{i}\Delta_0
\end{aligned} \qquad (39)$$

and the inhomogeneous vector I has nonzero components

$$I_1 = \Omega_0^*, \quad I_3 = \Omega_0. \qquad (40)$$

With the chosen notations, the fluorescence spectrum is given again by equations (34–36).

Of course, the inclusion of the additional driving fields and decay pathways and the incoherent pump processes changes the structure of the ideal spectrum discussed in Sections 2 and 3, but the differences are mainly quantitative unless the added decay rates become too large in comparison with the Rabi frequency Ω_0. With a careful selection of the atomic levels it should be possible to display evidence of the essential differences between the upper and lower level coupling, at least as quantum interference effects are concerned. As an example we show the fluorescence spectra from two identical sets of atoms with the same driving field Ω_0 applied to the transition 1–3 of Figure 1a and 1–2 of Figure 1b. In both cases a second weaker field is responsible for creating the initial state of excitation whose spontaneous emission yields the calculated spectrum. The results are shown in Figures 6 and 7, respectively, and are certainly quite different from each other in spite of the fact that all the parameters of the problem are identical in the two cases. Also, the qualitative similarity with the results shown in Figures 2 and 4 should be immediately apparent, in support of our previous claims to the effect that the inclusion of additional complications should not alter the appearance of interference effects to the point of making them unobservable.

From above discussion we can see that quantum interference exist in the case of upper level coupling, but it does not in the case of lower level coupling and its spectrum is the incoherent sum of two Lorentzian lines.

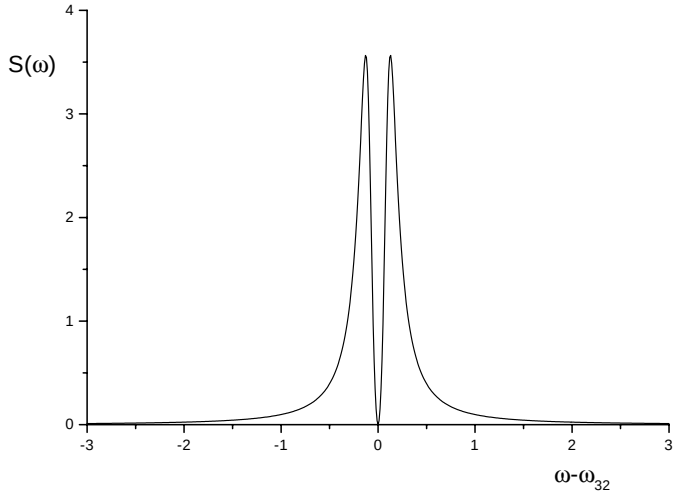

Fig. 6. Spontaneous emission spectrum $S(\omega)$ for the upper level coupling case with $\Omega_0 = 0.1$, $\Omega_1 = 0.001$, $\Delta_0 = \Delta_1 = 0$, $W_{21} = 0.01$, $W_{23} = 0.1$, $W_{31} = 0.01$, and $W_{32} = 0.1$.

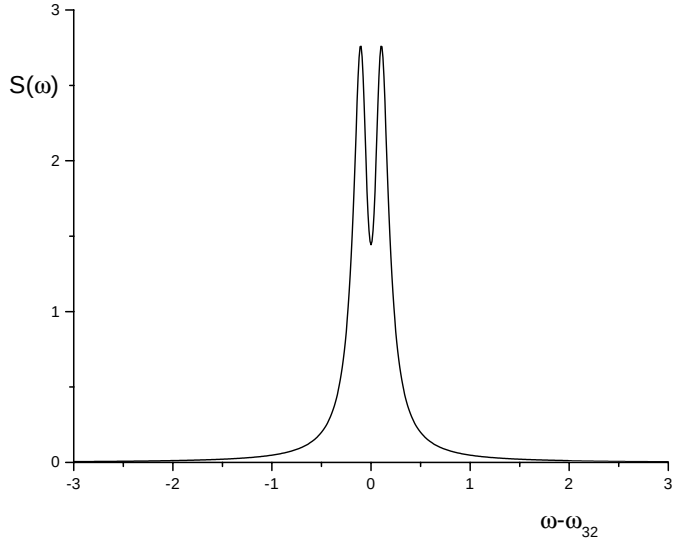

Fig. 7. Spontaneous emission spectrum $S(\omega)$ for the lower level coupling case with $\Omega_0 = 0.1$, $\Omega_1 = 0.001$, $\Delta_0 = \Delta_1 = 0$, $W_{21} = 0.01$, $W_{23} = 0.1$, $W_{31} = 0.01$, and $W_{32} = 0.1$.

If the spontaneous decay of the state 2 to 1 is included, the interference can appear in the lower level coupling. The transition of state 2 to 1 produces a new pathway, which makes the interference possible. The origin and the restoration of missing interference in emission is also studied by reference [14].

Appendix

The purpose of this appendix is to sketch the solution of the coupled amplitude equations (5) following a straightforward generalization of the Weisskopf-Wigner procedure [11]. We start by deriving explicit formal solutions of equation (5a)

$$C_{2j}(t) = C_{2j}(0) - g_j \int_0^t \mathrm{e}^{\mathrm{i}\delta_j t'} C_3(t')\mathrm{d}t'. \tag{A.1}$$

After imposing the initial conditions, substitution of equation (A.1) into equation (5b) yields

$$\dot{C}_3\ (t) = \Omega_0 \mathrm{e}^{-\mathrm{i}\Delta_0 t} C_1(t) + \sum_{j=1}^{\infty} g_j \mathrm{e}^{-\mathrm{i}\delta_j t} - g_j \int_0^t \mathrm{e}^{\mathrm{i}\delta_j t'} C_3(t')\mathrm{d}t'. \tag{A.2}$$

Next, we solve equation (A.2) along the lines of the traditional approach of Weisskopf and Wigner, with the result

$$\dot{C}_3\ (t) = \Omega_0 \mathrm{e}^{-\mathrm{i}\Delta_0 t} C_1(t) + \frac{1}{2}\gamma C_3(t) \tag{A.3}$$

where $\gamma = 2\pi D(\omega_{32}) g^2(\omega_{32})$, $D(\omega_{32})$ is the vacuum density of models calculated at the atomic transition frequency.

After replacing $C_3(t')$ on the right-hand side of equation (A.1) with the solution of equations (A.3, 5c), and carrying out the elementary integration, equation (7c) follow, in the longtime and infinite volume limits.

References

1. D.A. Cardimona, M.G. Raymer, C.R. Stroud, J. Phys. B **15**, 55 (1982).
2. M.O. Scully, S.Y. Zhu, A. Gavrielides, Phys. Rev. Lett. **62**, 2813 (1989).
3. S.E. Harris, Phys. Rev. Lett. **62**, 1033 (1989); S.Y. Zhu, Quant. Opt. **7**, 385 (1995).
4. P. Zhou, S. Swain, Phys. Rev. Lett. **77**, 3995 (1996).
5. S.Y. Zhu, M.O. Scully, Phys. Rev. Lett. **76**, 388 (1996); Hui-Rong Xia, Cen-Yun Ye, Shi-Yao Zhu, Phys. Rev. Lett. **77**, 1032 (1996).
6. P. Zhou, S. Swain, Phys. Rev. Lett. **78**, 832 (1997).
7. E. Paspalakis, P.L. Knight, Phys. Rev. Lett. **81**, 293 (1998).
8. E. Paspalakis, S.-Q. Gong, P.L. Knight, Opt. Commun. **152**, 293 (1998).
9. S. Menon, G.S. Agarwal, Phys. Rev. A **57**, 4014 (1998).
10. S.-Y. Zhu, L.M. Narducci, M.O. Scully, Phys. Rev. A **52**, 4791 (1995).
11. V. Weisskopf, E. Wigner, Z. Phys. **63**, 54 (1930); *ibid.* **65**, 18 (1931).
12. M. Lax, in *Statistical Physics, Phase Transitions, and Superfluidity*, edited by M. Chretien, E.P. Gross, S. Deser (Gordon and Breach, New York, 1968), Vol. 2, p. 265.
13. L.M. Narducci, M.O. Scully, G.-L. Oppo, P. Ru, J.R. Tredicce, Phys. Rev. A **43**, 3748 (1991).
14. G.S. Agarwal, Phys. Rev. A **58**, 686 (1998).